crystals

MDPI

Article

Two-Temperature Semiconductor Model Photomechanical and Thermal Wave Responses with Moisture Diffusivity Process

Abeer Alhashash [1], E. S. Elidy [2], A. A. El-Bary [3,4], Ramdan S. Tantawi [2] and Khaled Lotfy [2,*]

[1] Department of Mathematics, College of Science, Jouf University, Sakaka 24241, Saudi Arabia
[2] Department of Mathematics, Faculty of Science, Zagazig University, Zagazig P.O. Box 44519, Egypt
[3] Arab Academy for Science, Technology and Maritime Transport, Alexandria P.O. Box 1029, Egypt
[4] Department of Mathematics, Faculty of Science, Taibah University, Madinah 42353, Saudi Arabia
* Correspondence: khlotfy_1@yahoo.com

Abstract: In the context of the two-temperature thermoelasticity theory, a novel mathematical–physical model is introduced that describes the influence of moisture diffusivity in the semiconductor material. The two-dimensional (2D) Cartesian coordinate is used to study the coupling between the thermo-elastic plasma waves and moisture diffusivity. Dimensionless quantities are taken for the main physical fields with some initial conditions in the Laplace transform domain. The linear solutions are obtained analytically along with unknown variables when some conditions are loaded at the surface of the homogenous medium according to the two-temperature theory. The Laplace transform technique in inversion form is utilized with some numerical algebraic approximations in the time domain to observe the exact expressions. Due to the effects of the two-temperature parameter and moisture diffusivity, the numerical results of silicon material have been introduced. The impacts of thermoelectric, thermoelastic, and reference moisture parameters are discussed graphically with some physical explanations.

Keywords: photothermal theory; two temperature; moisture diffusivity; thermoelasticity; harmonic wave; semiconductor

Citation: Alhashash, A.; Elidy, E.S.; El-Bary, A.A.; Tantawi, R.S.; Lotfy, K. Two-Temperature Semiconductor Model Photomechanical and Thermal Wave Responses with Moisture Diffusivity Process. *Crystals* **2022**, *12*, 1770. https://doi.org/10.3390/cryst12121770

Academic Editor: Andreas Thissen

Received: 21 November 2022
Accepted: 28 November 2022
Published: 6 December 2022

1. Introduction

The spread of particles of one substance through those of another is called diffusion. Diffusion is the process by which concentrated liquids disperse when placed in water and by which odors disperse through the air. When particles disperse from places of high concentration, where there are many, to areas of low concentration, where there are fewer, diffusion occurs naturally. The interaction of moisture, heat, elastic, and electronic deformation can be seen in numerous engineering issues that are relevant to real-world applications. Mechanically applied additional stresses can significantly alter temperature and moisture distribution. As a consequence, there is a need to shed light on the relationship between mechanical deformation and diffusion induced by temperature and moisture.

An expanded theory of thermoelasticity put out by Lord and Shulman [1] substitutes a modified Fourier law that takes into account relaxation time parameters and a heat flux vector for the standard Fourier law. Another generalization of thermoelasticity was created by Green and Lindsay [2] using entropy inequality to place constraints on the governing equations. Sherief et al. [3] derived the variation principle for the governing equations and the equations for generalized thermoelasticity in an anisotropic medium. A new theory including energy dissipation in the propagation of thermal waves was put forth by Green and Nagdhi [4–6]. According to conductive temperature (ϕ) and thermodynamic temperature (T), Chen [7–9] created the two-temperature theory of thermoelasticity, which involves two temperature parameters (a). This hypothesis changed into the standard theory of heat conduction if (a) goes to zero [10].

A novel, generalized thermoelasticity model by Youssef [11] is based on two temperatures, T and ϕ, and it predicts that the temperature difference between the two is proportional to the heat supply $\ddot{\phi}_{ii}$ with a nonnegative constant a. Within the Dual Phase Lag (DPL) model framework, Ezzat et al. [12] created a two-temperature magneto thermoelastic fractional order model. The two-temperature thermoelastic theory with temperature rate dependence was developed by Shivay and Mukhopahyay [13] (TRDTT). The conductive and thermodynamic temperature dependency on temperature rate is a foundational element of this theory. To get the expression for thermodynamic and conductive temperature, the impact of two temperatures on wave thermo-mechanical loading is investigated [14]. Abouelregal and others [15] introduced the Moore–Gibson–Thomson equation and a new thermoelasticity model based on fractional calculus, Fourier's law of heat, and dual temperature theory was presented.

Sharma et al. [16] investigated the Rayleigh wave growth in an isotropic thermo-diffusive elastic half-plane. Aouadi [17] investigated the stability issues associated with a challenging thermoelastic diffusive problem. Lotfy and Hassan [18] employed normal mode analysis to examine the two-temperature theories in the generalized thermoelasticity. In the Dual Phase Lag Diffusion (DPLD) model setting, Kumar and Gupta [19] used the harmonic wave solution to get three coupled dilatational waves. The development of the Rayleigh wave in a thermoelastic half-plane with mass diffusion was studied by Kumar and Kansal [20–22]. The frequency equation for Rayleigh surface waves with mass diffusion in an isotropic thermodiffusive half-plane was developed by Kumar and Gupta [23]. We shall obtain a solution in the Fourier-transformed domain using the normal mode analysis technique. Applying the normal mode analysis requires making the assumption that all relationships are sufficiently smooth on the real axis to allow for the analysis of the normal modes of all these functions. The precise formulation for the temperature distribution, thermal stresses, and displacement components was obtained using the normal mode analysis [24–30]. When using two-temperature thermoelasticity with relaxation durations to study a variety of issues, Youssef and El-Bary [31] found that the outcomes are qualitatively distinct from those obtained when using one-temperature thermoelasticity. Fahmy et al. [32–36] studied the boundary element modeling and fractional boundary element solution of ultrasonic wave propagation according to the magneto-thermoviscoelastic medium in the context of the nonlinear generalized photothermal.

In the context of two-temperature theory, this paper investigates wave propagation in a photo-thermoelastic semiconductor medium under the effect of moisture using a moisture diffusivity model. When a photothermal transport process occurs at the free surface of a semi-infinite semiconducting medium, the problem is solved in two dimensions using thermoelasticity equations according to the moisture diffusivity. Finally, numerical computations have been carried out and graphically display when the inversion of Laplace transform is used.

2. Basic Equations

Assuming thermo-elastic semiconductor material has linear elastic properties and is transversely anisotropic homogeneous, the medium is examined during the photothermal transport phase, considering the overlap between plasma-thermal and moisture diffusion. The main four distributions are the carrier density (electronic diffusion) $N(r_i, t)$, moisture concentration $m(r_i, t)$, the temperature changes (thermal) $T(r_i, t)$, and the displacement vector (elastic) $u(r_i, t)$ (r_i represents the position vector and t represents the time). The interaction between plasma-thermal-elastic wave and moisture diffusion equations can be expressed in tensor form as follows [37–39]:

$$\frac{\partial N(r_i,t)}{\partial t} = D_E N_{,ii}(r_i,t) - \frac{N(r_i,t)}{\tau} + \kappa\, T(r_i,t) \tag{1}$$

$$\rho\, C_e(D_T\phi_{,ii} + D_T^m m_{,ii}) = \rho\, C_e\frac{\partial T}{\partial t} - \frac{E_g}{\tau}N + \gamma_t T_0\frac{\partial u_{i,j}}{\partial t} \tag{2}$$

$$k_m\left(D_m\, m_{,ii}(r_i,t) + D_m^T T_{,ii}(r_i,t)\right) = k_m\,\frac{\partial m(r_i,t)}{\partial t} - \frac{E_g}{\tau}N(r_i,t) + \gamma_m m_0 D_m\frac{\partial u_{i,j}(r_i,t)}{\partial t} \tag{3}$$

The motion equation in tensor form is written as follows:

$$\rho\,\frac{\partial^2 u_i(r_i,t)}{\partial t^2} = \sigma_{ij,j} \tag{4}$$

The equation of the strain is:

$$\varepsilon_{ij} = \frac{1}{2}(u_{i,j} + u_{j,i}) \tag{5}$$

According to the two-temperature theory, the relationship between the heat conduction temperature and the thermo-dynamical heat temperature is as follows:

$$\phi - T = a\,\phi_{,ii} \tag{6}$$

where a is a two-temperature positive parameter (chosen). The general stress-tensor form with moisture concentration is:

$$\sigma_{ij} = C_{ijkl}\varepsilon_{kl} - \beta_{ij}(\alpha_t T + d_n N) - \beta_{ij}^m\, m, \quad i,j,k,l = 1,2,3 \tag{7}$$

where D_T expresses temperature diffusivity, D_m is the diffusion coefficient of moisture, D_T^m and D_m^T are coupled diffusivities, D_E is the carrier diffusion coefficient, m_0 reference moisture, k_m moisture diffusivity, C_{ijkl} represents the isothermal parameters tensor of an elastic medium, ε_{kl} is the strain tensor, and β_{ij} and β_{ij}^m are the isothermal thermoelastic coupling tensor material coefficient of moisture concentration, respectively. The thermal activation coupling is $\kappa = \frac{\partial N_0}{\partial T}\frac{T}{\tau}$, N_0 represents the equilibrium carrier concentration [33,35]. The quantities E_g, ρ, τ, (λ, μ), and T_0 are the energy gap, the density, the lifetime, Lame's elastic constants, and the reference temperature, respectively. On the other hand, $\gamma_t = (3\lambda + 2\mu)\alpha_T$ is the volume thermal expansion, α_T the linear thermal expansion coefficient, C_e the specific heat parameter, and δ_n the difference between conductive deformation potential and valence band.

These are the 2D definitions of the physical quantities:

$$\frac{\partial N}{\partial t} = D_E\nabla^2 N - \frac{N}{\tau} + \kappa\, T \tag{8}$$

$$\rho\, C_e\left(D_T\nabla^2\phi + D_T^m\nabla^2 m\right) = \rho\, C_e\frac{\partial T}{\partial t} - \frac{E_g}{\tau}N + \gamma_t\, T_0\frac{\partial}{\partial t}\left(\frac{\partial u}{\partial x} + \frac{\partial w}{\partial z}\right) \tag{9}$$

$$k_m\left(D_m\nabla^2 m + D_m^T\nabla^2 T\right) = k_m\frac{\partial m}{\partial t} - \frac{E_g}{\tau}N + \gamma_m\, m_0 D_m\frac{\partial}{\partial t}\left(\frac{\partial u}{\partial x} + \frac{\partial w}{\partial z}\right) \tag{10}$$

The motion Equation (4) has the following structure:

$$\rho\,\frac{\partial^2 u}{\partial t^2} = (2\mu + \lambda)\frac{\partial^2 u}{\partial x^2} + \mu\frac{\partial^2 u}{\partial z^2} - \gamma_t\frac{\partial T}{\partial x} - \delta_n\frac{\partial N}{\partial x} - \gamma_m\frac{\partial m}{\partial x} \tag{11}$$

$$\rho\,\frac{\partial^2 w}{\partial t^2} = (2\mu + \lambda)\frac{\partial^2 w}{\partial z^2} + \mu\frac{\partial^2 w}{\partial x^2} - \gamma_t\frac{\partial T}{\partial z} - \delta_n\frac{\partial N}{\partial z} - \gamma_m\frac{\partial m}{\partial z} \tag{12}$$

where $\gamma_{t,m} = \beta\,\alpha_{m,T}$ and $\delta_n = \beta d_n, \beta = 3\mu + 2\lambda$, $\nabla^2 = \frac{\partial^2}{\partial x^2} + \frac{\partial^2}{\partial z^2}$.

According to the two-temperature Equation (7), yields:

$$\phi - T = a\nabla^2\phi \tag{13}$$

The 2D constitutive equation has the following structure:

$$\sigma_{xx} = (2\mu + \lambda)\frac{\partial u}{\partial x} + \lambda\frac{\partial w}{\partial z} - \beta(\alpha_t T + d_n N) - \gamma_m m \tag{14}$$

$$\sigma_{zz} = (2\mu + \lambda)\frac{\partial w}{\partial z} + \lambda\frac{\partial u}{\partial x} - \beta(\alpha_t T + d_n N) - \gamma_m m \tag{15}$$

$$\sigma_{xz} = \mu(\frac{\partial u}{\partial z} + \frac{\partial w}{\partial x}) - \gamma_m m \tag{16}$$

3. Formulation of the Problem

We can add two scalar potential functions in their non-dimensional form as: $u = \frac{\partial \Pi}{\partial x} + \frac{\partial \Psi}{\partial z}$ and $w = \frac{\partial \Pi}{\partial z} - \frac{\partial \Psi}{\partial x}$. For more simplicity, the non-dimensional variants are introduced:

$$\begin{gathered}(x', z', u', w') = \tfrac{(x,z,u,w)}{C_T t^*},\ t' = \tfrac{t}{t^*} \\ ((T', \phi'), N') = \tfrac{(\gamma_t (T,\phi), \delta_n N)}{2\mu + \lambda},\ \sigma' = \tfrac{\sigma}{\mu},\ e' = e,\ m' = m\end{gathered} \tag{17}$$

In the above equations, the dash is removed for convenience, yields:

$$(\nabla^2 - q_1 - q_2\frac{\partial}{\partial t})N + \varepsilon_3\, T = 0 \tag{18}$$

$$\nabla^2\phi - a_1\frac{\partial}{\partial t}T + a_2\nabla^2 m + a_3\, N - \varepsilon_1\frac{\partial}{\partial t}\nabla^2\Pi = 0 \tag{19}$$

$$\left(\nabla^2 - a_4\frac{\partial}{\partial t}\right)m + a_5\nabla^2 T + a_6\, N - a_7\nabla^2\Pi = 0 \tag{20}$$

$$\left(\nabla^2 - \frac{\partial^2}{\partial t^2}\right)\Pi - T - N - a_8 m = 0 \tag{21}$$

$$\left\{\nabla^2 - \alpha\frac{\partial^2}{\partial t^2}\right\}\Psi = 0 \tag{22}$$

$$\phi - T = \alpha_6\nabla^2\phi \tag{23}$$

The stress component takes the following form in the non-dimensional form:

$$\sigma_{xx} = a_9\frac{\partial^2\Pi}{\partial x^2} + a_{10}\frac{\partial^2\Pi}{\partial z^2} + 2\frac{\partial^2\Psi}{\partial z\partial x} - a_9(T + N)) - a_{11} m \tag{24}$$

$$\sigma_{zz} = a_9\frac{\partial^2\Pi}{\partial z^2} + a_{10}\frac{\partial^2\Pi}{\partial x^2} - 2\frac{\partial^2\Psi}{\partial z\partial x} - a_9(T + N) - a_{11} m \tag{25}$$

$$\sigma_{xz} = \frac{\partial^2\Psi}{\partial z^2} + 2\frac{\partial^2\Pi}{\partial x\partial z} - \frac{\partial^2\Psi}{\partial x^2} \tag{26}$$

where

$$
\begin{aligned}
&q_1 = \frac{kt^*}{D_E\rho\tau C_e} \quad q_2 = \frac{k}{D_E\rho C_e} \quad a_1 = \frac{C_T^2 t^*}{D_T} \quad a_2 = \frac{D_T^m \gamma_t}{D_T(2\mu+\lambda)} \\
&a_3 = \varepsilon_2 a_1 \\
&a_4 = \frac{C_T^2 t^*}{D_m} \quad a_5 = \frac{D_m^T(2\mu+\lambda)}{D_m\gamma_t} \quad a_6 = \frac{E_g(2\mu+\lambda)t^* a_4}{k_m\delta_n\tau} \quad a_7 = \frac{\gamma_m m_0 C_T^2 t^*}{k_m} \\
&a_8 = \frac{\gamma_m}{2\mu+\lambda} \quad a_9 = \frac{2\mu+\lambda}{\mu} \quad a_{10} = \frac{\lambda}{\mu} \quad a_{11} = \frac{\gamma_m}{\mu} \\
&\varepsilon_1 = \frac{\gamma_t^2 T_0 t^*}{k\rho} \\
&\varepsilon_2 = \frac{\alpha_T E_g t^*}{\tau d_n \rho C_e} \quad \varepsilon_3 = \frac{d_n k\kappa t^*}{\alpha_T \rho C_e D_E} \\
&C_T^2 = \frac{2\mu+\lambda}{\rho}, \; \delta_n = (2\mu + 3\lambda)d_n \\
&t^* = \frac{k}{\rho C_e C_T^2} \\
&\alpha_6 = \frac{a}{t^{*2} C_T^2}, \; \alpha = \frac{K}{\mu C_e}
\end{aligned}
$$

where ε_1, ε_2, and ε_3 can be called the thermoelastic coupling parameter, the thermo-energy coupling parameter, and the thermoelectric coupling parameter, respectively.

4. Harmonic Wave Analysis

Using the harmonic wave approach, the basic physical fields in 2D solutions are dissected and can be produced for any function (normal mode analysis) in the manner of [22]:

$$G(x,z,t) = \overline{G}(x)\exp(\omega t + ibz) \tag{27}$$

where the function $\overline{G}(x)$ represents the amplitude of the basic physical quantity $G(x,z,t)$, $i = \sqrt{1}$, ω presents the complex time frequency, and expresses b the wave number in the z-direction. Equations (18)–(26) are solved using the normal mode approach, which is defined in Equation (27) and results in [25]:

$$(D^2 - \alpha_1)\overline{N} + \varepsilon_3\,\overline{T} = 0 \tag{28}$$

$$(D^2 - b^2)\overline{\phi} - \alpha_2\,\overline{T} + a_2(D^2 - b^2)\,\overline{m} + a_3\,\overline{N} - \alpha_3\,(D^2 - b^2)\overline{\Pi} = 0 \tag{29}$$

$$\left(D^2 - \alpha_4\right)\overline{m} + a_5(D^2 - b^2)\,\overline{T} + a_6\,\overline{N} - \alpha_5\,(D^2 - b^2)\overline{\Pi} = 0 \tag{30}$$

$$(D^2 - \alpha_6)\overline{\Pi} - \overline{T} - \overline{N} - a_8\,\overline{m} = 0 \tag{31}$$

$$(D^2 - \alpha_7)\overline{\phi} + \beta\overline{T} = 0 \tag{32}$$

$$\left\{D^2 - \alpha_8\right\}\overline{\Psi} = 0 \tag{33}$$

$$\overline{\sigma}_{xx} = \left(a_9 D^2 - a_{10}b^2\right)\overline{\Pi} + 2ibD\overline{\Psi} - a_9\left(\overline{T} + \overline{N}\right)) - a_{11}\overline{m} \tag{34}$$

$$\overline{\sigma}_{zz} = \left(a_{10}D^2 - a_9 b^2\right)\overline{\Pi} - 2ibD\overline{\Psi} - a_9\left(\overline{T} + \overline{N}\right) - a_{11}\overline{m} \tag{35}$$

$$\overline{\sigma}_{xz} = -(D^2 - b^2)\overline{\Psi} + 2ibD\overline{\Pi} \tag{36}$$

where $D = \frac{d}{dx}$, $\alpha_1 = b^2 + q_1 + q_2\omega$, $\alpha_2 = a_1\omega$, $\alpha_3 = \omega\varepsilon_1$, $\alpha_4 = a_4\omega + b^2$, $\alpha_5 = a_7\omega$, $\alpha_6 = b^2 + \omega^2$, $\alpha_7 = b^2 + \beta\beta = \frac{1}{a^*}$.

Eliminating $\overline{\phi}, \overline{T}, \overline{\Pi}, \overline{N}$, and $\overline{m}$ between Equations (28)–(31), and (32) yields:

$$(D^{10} - \Theta_1 D^8 + \Theta_2 D^6 - \Theta_3 D^4 + \Theta_4 D^2 - \Theta_5)\left\{\overline{\phi}, \overline{m}, \overline{N}, \overline{T}, \overline{\Pi}\right\}(x)e^{(\omega t + ibz)} = 0 \tag{37}$$

where

$$
\begin{aligned}
&\Theta_1 = \tfrac{(-2b^2 a_2 a_5 - a_2 a_5 \alpha_1 - a_2 a_5 \alpha_6 - a_2 a_5 \alpha_7 - a_5 a_8 \alpha_3 - a_2 \alpha_5 + \beta + \alpha_2 + \alpha_3)}{(-a_2 a_5)},\\
&\Theta_2 = \tfrac{1}{(a_2 a_5)}\left\{\begin{array}{l} b^4 a_2 a_5 + 2b^2 a_2 a_5 \alpha_1 + 2b^2 a_2 a_5 \alpha_6 + 2b^2 a_2 a_5 \alpha_7 + 2b^2 a_5 a_8 \alpha_3 + 2b^2 a_2 \alpha_5 + \\ a_2 a_5 \alpha_1 \alpha_6 + a_2 a_5 \alpha_1 \alpha_7 + a_2 a_5 \alpha_6 \alpha_7 + a_5 a_8 \alpha_1 \alpha_3 + a_5 a_8 \alpha_3 \alpha_7 \\ -b^2 \beta - b^2 \alpha_3 - \beta a_8 \alpha_5 - a_2 a_7 \varepsilon_3 + a_2 \alpha_1 \alpha_5 + a_2 \alpha_5 \alpha_7 + a_2 \alpha_5 \varepsilon_3 - a_8 \alpha_2 \alpha_5 \\ -\beta \alpha_1 - \beta \alpha_4 - \beta \alpha_6 + a_3 \varepsilon_3 - \alpha_1 \alpha_2 - \alpha_1 \alpha_3 - \alpha_2 \alpha_4 - \alpha_2 \alpha_6 - \alpha_2 \alpha_7 - \alpha_3 \alpha_4 - \alpha_3 \alpha_7 - \alpha_3 \varepsilon_3 \end{array}\right\},\\
&\Theta_3 = \tfrac{-1}{(a_2 a_5)}\left\{\begin{array}{l} -b^4 a_2 a_5 \alpha_1 - b^4 a_2 a_5 \alpha_6 - b^4 a_2 a_5 \alpha_7 - b^4 a_5 a_8 \alpha_3 - b^4 a_2 \alpha_5 - 2b^2 a_2 a_5 \alpha_1 \alpha_6 - \\ 2b^2 a_2 a_5 \alpha_1 \alpha_7 - 2b^2 a_2 a_5 \alpha_6 \alpha_7 - 2b^2 a_5 a_8 \alpha_1 \alpha_3 - 2b^2 a_5 a_8 \alpha_3 \alpha_7 + 2b^2 \beta a_8 \alpha_5 \\ +b^2 a_2 a_7 \varepsilon_3 - 2b^2 a_2 \alpha_1 \alpha_5 - 2b^2 a_2 \alpha_5 \alpha_7 - 2b^2 a_2 \alpha_5 \varepsilon_3 + b^2 a_8 \alpha_2 \alpha_5 - a_2 a_5 \alpha_1 \alpha_6 \alpha_7 \\ -a_5 a_8 \alpha_1 \alpha_3 \alpha_7 + b^2 \beta \alpha_1 + b^2 \beta \alpha_4 + b^2 \beta \alpha_6 + b^2 \alpha_1 \alpha_3 + b^2 \alpha_3 \alpha_4 + b^2 \alpha_3 \alpha_7 + \\ b^2 \alpha_3 \varepsilon_3 + \beta a_8 \alpha_1 \alpha_5 + a_2 a_7 \alpha_6 \varepsilon_3 + a_2 a_7 \alpha_7 \varepsilon_3 - a_2 \alpha_1 \alpha_5 \alpha_7 - a_2 \alpha_5 \alpha_7 \varepsilon_3 - a_2 a_8 \alpha_5 \varepsilon_3 + \\ a_7 a_8 \alpha_3 \varepsilon_3 + a_8 \alpha_1 \alpha_2 \alpha_5 + a_8 \alpha_2 \alpha_5 \alpha_7 + \beta \alpha_1 \alpha_4 + \beta \alpha_1 \alpha_6 + \beta \alpha_4 \alpha_6 - a_3 \alpha_4 \varepsilon_3 - a_3 \alpha_6 \varepsilon_3 - \\ a_3 \alpha_7 \varepsilon_3 + \alpha_1 \alpha_2 \alpha_4 + \alpha_1 \alpha_2 \alpha_6 + \alpha_1 \alpha_2 \alpha_7 + \alpha_1 \alpha_3 \alpha_4 + \alpha_1 \alpha_3 \alpha_7 + \alpha_2 \alpha_4 \alpha_6 + \alpha_2 \alpha_4 \alpha_7 \\ +\alpha_2 \alpha_6 \alpha_7 + \alpha_3 \alpha_4 \alpha_7 + \alpha_3 \alpha_4 \varepsilon_3 + \alpha_3 \alpha_7 \varepsilon_3 \end{array}\right\},\\
&\Theta_4 = \tfrac{1}{(a_2 a_5)}\left\{\begin{array}{l} b^4 a_2 a_5 \alpha_1 \alpha_6 + b^4 a_2 a_5 \alpha_1 \alpha_7 + b^4 a_2 a_5 \alpha_6 \alpha_7 + b^4 a_5 a_8 \alpha_1 \alpha_3 + b^4 a_5 a_8 \alpha_3 \alpha_7 - b^4 \beta a_8 \alpha_5 + \\ b^4 a_2 \alpha_1 \alpha_5 + b^4 a_2 \alpha_5 \alpha_7 + b^4 a_2 \alpha_5 \varepsilon_3 + 2b^2 a_2 a_5 \alpha_1 \alpha_6 \alpha_7 + 2b^2 a_5 a_8 \alpha_1 \alpha_3 \alpha_7 - 2b^2 \beta a_8 \alpha_1 \alpha_5 \\ -b^2 a_2 a_7 \alpha_6 \varepsilon_3 - b^2 a_2 a_7 \alpha_7 \varepsilon_3 + 2b^2 a_2 \alpha_1 \alpha_5 \alpha_7 + 2b^2 a_2 \alpha_5 \alpha_7 \varepsilon_3 + b^2 a_3 a_8 \alpha_5 \varepsilon_3 - b^2 a_7 a_8 \alpha_3 \varepsilon_3 \\ -b^2 a_8 \alpha_1 \alpha_2 \alpha_5 - b^2 a_8 \alpha_2 \alpha_5 \alpha_7 - b^2 \beta \alpha_1 \alpha_4 - b^2 \beta \alpha_1 \alpha_6 - b^2 \beta \alpha_4 \alpha_6 - b^2 \alpha_1 \alpha_3 \alpha_4 - b^2 \alpha_1 \alpha_3 \alpha_7 \\ -b^2 \alpha_3 \alpha_4 \alpha_7 - b^2 \alpha_3 \alpha_4 \varepsilon_3 - b^2 \alpha_3 \alpha_7 \varepsilon_3 - a_2 a_7 \alpha_6 \alpha_7 \varepsilon_3 + a_3 a_8 \alpha_5 \alpha_7 \varepsilon_3 - a_7 a_8 \alpha_3 \alpha_7 \varepsilon_3 - \\ a_8 \alpha_1 \alpha_2 \alpha_5 \alpha_7 - \beta \alpha_1 \alpha_4 \alpha_6 + a_3 \alpha_4 \alpha_6 \varepsilon_3 + a_3 \alpha_4 \alpha_7 \varepsilon_3 + a_3 \alpha_6 \alpha_7 \varepsilon_3 - \alpha_1 \alpha_2 \alpha_4 \alpha_6 - \alpha_1 \alpha_2 \alpha_4 \alpha_7 \\ -\alpha_1 \alpha_2 \alpha_6 \alpha_7 - \alpha_1 \alpha_3 \alpha_4 \alpha_7 - \alpha_2 \alpha_4 \alpha_6 \alpha_7 - \alpha_3 \alpha_4 \alpha_7 \varepsilon_3 \end{array}\right\},\\
&\Theta_5 = \tfrac{-1}{(a_2 a_5)}\left\{\begin{array}{l} -b^2 \alpha_1 \alpha_3 \alpha_7 - b^2 \alpha_3 \alpha_4 \alpha_7 - b^2 \alpha_3 \alpha_4 \varepsilon_3 - b^2 \alpha_3 \alpha_7 \varepsilon_3 - a_2 a_7 \alpha_6 \alpha_7 \varepsilon_3 + a_3 a_8 \alpha_5 \alpha_7 \varepsilon_3 \\ -a_7 a_8 \alpha_3 \alpha_7 \varepsilon_3 - a_8 \alpha_1 \alpha_2 \alpha_5 \alpha_7 - \beta \alpha_1 \alpha_4 \alpha_6 + a_3 \alpha_4 \alpha_6 \varepsilon_3 + a_3 \alpha_4 \alpha_7 \varepsilon_3 + a_3 \alpha_6 \alpha_7 \varepsilon_3 \\ -\alpha_1 \alpha_2 \alpha_4 \alpha_6 - \alpha_1 \alpha_2 \alpha_4 \alpha_7 - \alpha_1 \alpha_2 \alpha_6 \alpha_7 - \alpha_1 \alpha_3 \alpha_4 \alpha_7 - \alpha_2 \alpha_4 \alpha_6 \alpha_7 - \alpha_3 \alpha_4 \alpha_7 \varepsilon_3 \end{array}\right\}.
\end{aligned} \tag{38}
$$

The principle ordinary differential equation (ODE) was fixed by the factorization method in the manner described in (37):

$$\left(D^2 - m_1^2\right)\left(D^2 - m_2^2\right)\left(D^2 - m_3^2\right)\left(D^2 - m_4^2\right)\left(D^2 - m_5^2\right)\{\ \overline{\phi}, \overline{T}, \overline{\Pi}, \overline{N}, \overline{m}\ \}(x)\, e^{(\omega t + ibz)} = 0 \tag{39}$$

where $m_n^2 (n = 1, 2, 3, 4, 5)$ represent the roots when $x \to \infty$. The following is the form that the solution to Equation (ODE) (39) takes (according to the linearity of the problem):

$$\overline{T}(x) = \sum_{n=1}^{5} D_n(b, \omega)\, e^{-m_n x} \tag{40}$$

The solutions of the other values can be represented similarly as:

$$\overline{N}(x) = \sum_{n=1}^{5} D'_n(b, \omega)\, e^{-m_n x} = \sum_{n=1}^{5} H_{1n} D_n(b, \omega)\, e^{-m_n x} \tag{41}$$

$$\overline{\Pi}(x) = \sum_{n=1}^{5} D''_n(b, \omega)\, \exp(-m_n x) = \sum_{n=1}^{5} H_{2n}\, D_n(b, \omega)\, \exp(-m_n x) \tag{42}$$

$$\overline{m}(x) = \sum_{n=1}^{5} D'''_n\,(b, \omega)\, \exp(-m_n x) = \sum_{n=1}^{5} H_{3n}\, D_n(b, \omega)\, \exp(-m_n x) \tag{43}$$

$$\overline{\phi}(x) = \sum_{n=1}^{5} D_n^{(4)}(b, \omega)\, \exp(-m_n x) = \sum_{n=1}^{5} H_{4n}\, D_n(b, \omega)\, \exp(-m_n x) \tag{44}$$

The following form represents the solution to equation:

$$\overline{\psi}(x) = D_6(b, \omega)\, e^{-m_6 x} \tag{45}$$

where $m_6 = \pm\sqrt{\alpha_8}$ are the real roots of Equation (33). The displacement components can first be represented in terms of parameters in accordance with Equation (18) to produce the stress components:

$$\overline{\sigma}_{xx} = \sum_{n=1}^{5} H_{5n}\, D_n(b,\omega)\ \exp(-m_n x) - 2ibm_6 D_6 \exp(-m_6 x) \tag{46}$$

$$\overline{\sigma}_{zz} = \sum_{n=1}^{5} H_{6n}\, D_n(b,\omega)\ \exp(-m_n x) + 2ibm_6 D_6 \exp(-m_6 x) \tag{47}$$

$$\overline{\sigma}_{xz} = \sum_{n=1}^{5} H_{7n} D_n(b,\omega)\ \exp(-m_n x) - (\,m_6^2 + b^2) D_6 \exp(-m_6 x) \tag{48}$$

Since

$$\overline{u}(x) = D\overline{\Pi} + i\, b\overline{\psi} \tag{49}$$

$$\overline{w}(x) = i\, b\overline{\Pi} - D\,\overline{\psi} \tag{50}$$

Then,

$$\overline{u}(x) = \sum_{n=1}^{5} D_n''(b,\omega)\, m_n e^{-m_n x} + ibD_6(b,\omega)\ \exp(-m_6 x) \tag{51}$$

$$\overline{w}(x) = ib\sum_{n=1}^{5} D_n''(b,\omega)\, e^{-m_n x} + D_6(b,\omega)\, m_6 \exp(-m_6 x) \tag{52}$$

where $D_n, D_n', D_n''\ , D_n'''\ ,$ and $D_n^{(4)}\ \ , n = 1,2,3,4,5$ are unknown parameters depending on the parameter b,ω. The relationship between the unknown parameters $D_n, D_n', D_n''\ , D_n'''\ ,$ and $D_n^{(4)}\ \ , n = 1,2,3,4,5$ can be obtained when using the main Equations (28)–(35) and (36), which take the following relationship:

$$\begin{gathered}
H_{1n} = \frac{-\varepsilon_3}{{m_n}^2 - \alpha_1} \\
H_{2n} = \frac{(a_5a_8 - 1)m_n^4 + (-b^2a_5a_8 - a_5a_8\alpha_1 + \alpha_1 + \alpha_4 + \varepsilon_3)m_n^2 + b^2a_5a_8\alpha_1 - a_7a_8\varepsilon_3 - \alpha_1\alpha_4 - \alpha_4\varepsilon_3}{m_n^6 + (-a_8\alpha_5 - \alpha_1 - \alpha_4 - \alpha_6)\, m_n^4 + (b^2a_8\alpha_5 + a_8\alpha_1\alpha_5 + \alpha_1\alpha_4 + \alpha_1\alpha_6 + \alpha_6\alpha_4)m_n^2 - b^2a_8\alpha_1\alpha_5 - \alpha_1\alpha_4\alpha_6}, \\
H_{3n} = -\frac{(m_n^6 + (-s^2 - \alpha_1 - \alpha_2 - \alpha_3)m_n^4 + (s^2\alpha_1 + s^2\alpha_2 - a_3\varepsilon_3 + \alpha_1\alpha_2 + \alpha_1\alpha_3 + \alpha_3\varepsilon_3)m_n^2 + s^2a_3\varepsilon_3 - s^2\alpha_1\alpha_2)}{((m_n^2 - \alpha_1)(m_n^2a_2 - s^2a_2 - a_8\alpha_3)m_n^2)} \\
H_{4n} = \frac{-\beta}{({m_n}^2 - \alpha_7)} \\
H_{5n} = \left(a_9m_n^2\ -\ a_{10}b^2\right)H_{2n}\ -\ a_9((\,1\ +\ H_{1n}))\ -\ a_{11}H_{3n} \\
H_{6n} = \left(a_9m_n^2\ -\ a_{10}b^2\right)H_{2n}\ -\ a_9((\,1\ +\ H_{1n}))\ -\ a_{11}H_{3n} \\
H_{6n} = 2I\, b\, m_i\, H_{3i}
\end{gathered} \tag{53}$$

5. Applications

In this section, we determine the parameters $D_n(n = 1,2,3,4,5,6)$. We should suppress the unbounded positive exponentials at infinity in the physical problem. The constants $D_1,\ D_2,\ D_3,\ D_4, D_5,$ and D_6 must be selected so that the boundary conditions on the surface $x = 0$ (near the vacuum) take the form [40]:

(i) Mechanical boundary condition that the surface of the half-space is traction load

$$\sigma_{xx}(0,\, z,\, t) = \ -p_1 \exp(\omega t + ibz) \tag{54}$$

(ii) The half-space's surface must be traction-free as a displacement boundary condition:

$$u(0,z,t) = 0. \tag{55}$$

(iii) Assuming that the boundary $x = 0$ is thermally insulated, we have

$$\frac{\partial T(0,z,t)}{\partial x} = 0. \tag{56}$$

(iv) The carriers have a limited chance of recombining when they reach the sample surface during the diffusion process. Therefore, the following can be the carrier density's boundary condition:

$$\frac{\partial N(0,z,t)}{\partial x} = \frac{s}{D_e}N. \tag{57}$$

(v) The moisture diffusion condition at the free boundary surface $x = 0$ is:

$$m(0,z,t) = 0. \tag{58}$$

(viii) The conductive temperature condition at the free boundary surface $x = 0$ is:

$$\phi(0,z,t) = \phi_0. \tag{59}$$

6. Numerical Results and Discussions

Temperature, displacement, moisture concentration, carrier density (electronic diffusion), conductive temperature, and normal distribution of stress are some of the physical quantities with numerical values that are calculated for this problem. Utilizing materials, the numerical simulation is carried out. The constants have been utilized in S.I. The plot is made using the unit and the MATLAB program. Table 1 lists the physical constants for Si and Ge for the lower medium [40]:

Table 1. Physical parameters of Si and Ge materials.

Units	Symbol	Si	Ge
	λ	6.4×10^{10}	0.48×10^{11}
N/m^2	μ	6.5×10^{10}	0.53×10^{11}
kg/m^3	ρ	2330	5300
K	T_0	800	723
s	τ	5×10^{-5}	1.4×10^{-6}
m^2/s	D_E	2.5×10^{-3}	10^{-2}
m^3	d_n	-9×10^{-31}	-6×10^{-31}
eV	E_g	1.11	0.72
K^{-1}	α_t	4.14×10^{-6}	3.4×10^{-3}
$Wm^{-1}K^{-1}$	k	150	60
$J/(kg\,K)$	C_e	695	310
m/s	s	2	2
	D_T	$\frac{k}{\rho C_e}$	$\frac{k}{\rho C_e}$
$(m^2(\%H_2O)/s(K))$	D_T^m	2.1×10^{-7}	2.1×10^{-7}
$(m^2 s(K)/(\%H_2O))$	D_m^T	0.648×10^{-6}	0.648×10^{-6}
Reference moisture	m_0	10%	10%
$m^2 s^{-1}$	D_m	0.35×10^{-2}	0.35×10^{-2}
$cm/cm(\%H_2O)$	α_m	2.68×10^{-3}	2.68×10^{-3}
(kg/msM)	k_m	2.2×10^{-8}	2.2×10^{-8}

6.1. The Effect of Two-Temperature Parameter

In the case of moisture diffusivity, the first group (Figure 1) depicts how the primary fields in this phenomenon vary depending on the various values of the two-temperature parameter measured against the horizontal distance x. This category includes two cases, the first of which is when the two-temperature parameter does not disappear when $a \neq 0$. The one-temperature example applies here because the thermodynamic and conductive temperatures are equal. The two-temperature hypothesis is obtained in contrast when $a > 0$. According to Figure 1, the carrier density in the two-temperature case and the one-temperature wave propagation exhibit the same behavior. The wave propagations have a different behavior in the other distributions (thermodynamic temperature, displacement, stress, and conductive temperature). The magnitude of all field distributions from this category is greatly influenced by the two-temperature parameter. In two instances of a two-temperature parameter, the physical fields meet the surface boundary criteria.

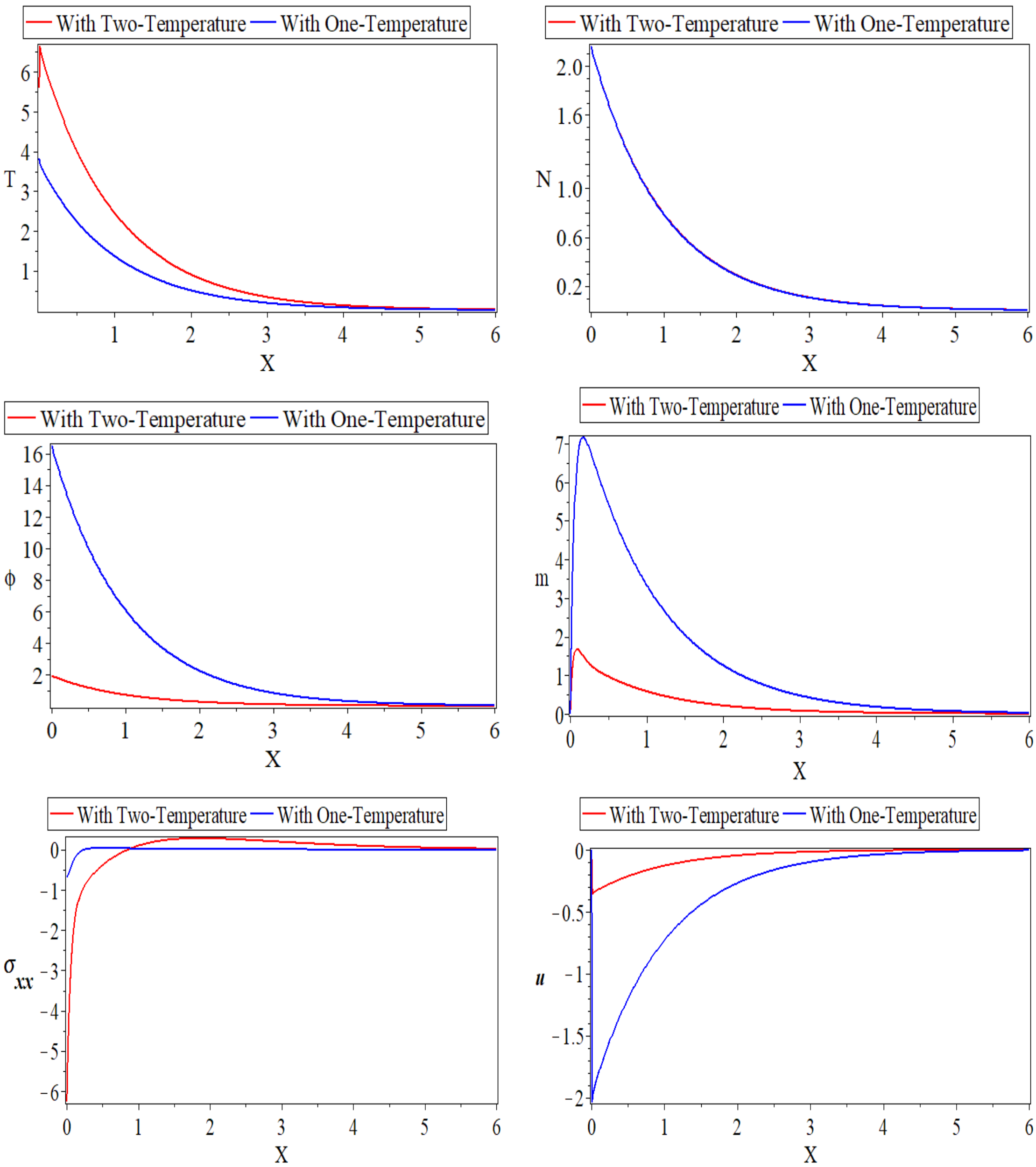

Figure 1. Represents the variations of main fields in this phenomenon according to the different values of two-temperature parameter under the effect of moisture field.

6.2. The Impact of Thermoelastic Coupling Parameter

Figure 2 (in the second category) displays the primary physical fields against the horizontal distance within the framework of photo-thermoelasticity theory with moisture diffusivity inside the two-temperature theory. All calculations are made under the moisture diffusivity when $\varepsilon_3 = -7.8 \times 10^{-36}$ and $m_0 = 10\%$ for Si material. The different types of the thermoelastic coupling parameter are discussed in each subfigure. The solid lines (———) represent the case when $\varepsilon_1 = 0.001$, the dashed lines (— — —) express the case at $\varepsilon_1 = 0.002$, and the dotted lines (⋯⋯⋯) show the case at $\varepsilon_1 = 0.003$. The thermodynamic temperature distribution (T) is shown in the first subfigure along with how the distance affects the dimensionless thermoelastic coupling parameters. Starting from a positive minimum temperature that satisfies the thermally insulated requirement, the thermodynamic temperature T rises rapidly in the first range until it reaches the maximum peak temperature close to the surface due to photo-excitation and moisture diffusivity. The distribution, on the other hand, shrinks in the second range to arrive at the minimum value distant from the surface. The electronic diffusive distribution is shown against the distance in variation values of the thermoelastic parameters in the second subfigure. However, the carrier density, which exhibits a similar quality characteristic, is not significantly affected by a slight change in the thermoelastic coupling parameters. The fourth subfigure describes the moisture concentration m distribution versus the horizontal distance x, while the third subfigure depicts the conductive temperature, which exhibits the same behavior as the first subfigure. For all three cases, the distribution of moisture content starts at zero. The distribution adopts an exponential pattern with smooth decrementing with $\varepsilon_1 = 0.001$. On the other hand, due to moisture diffusivity, when $\varepsilon_1 = 0.002$ and $\varepsilon_1 = 0.003$ the distribution of moisture concentration dramatically declines in the first range, and it adopts exponential propagation behavior until it reaches a minimum value close to the zero line. The fifth subfigure shows how the amplitude of the stress force σ is increasing as a result of the mechanical loads' tendency to raise the thermoelastic coupling parameters' values. The displacement distribution with horizontal distance caused by moisture diffusivity and the thermal impact of photothermal stimulation for the rough surface is shown in the sixth subfigure. For all three thermoelastic coupling parameter scenarios, the displacement distribution begins at zero and climbs to maximum values close to the surface before decreasing exponentially until it approaches a minimum value close to the zero line [41]. These results are in agreement with what has been observed through practical experiments [42,43].

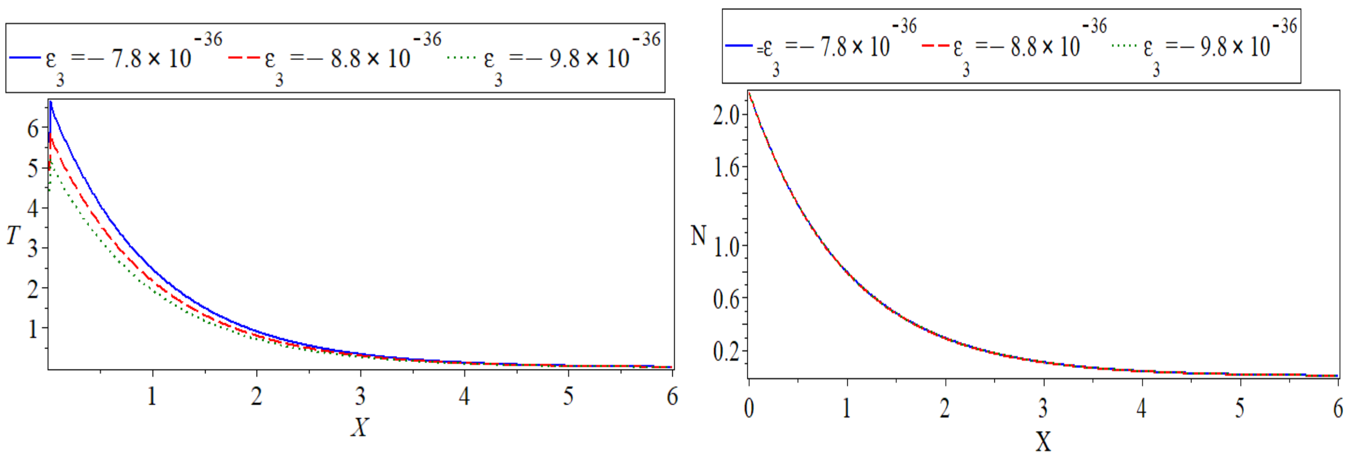

Figure 2. *Cont.*

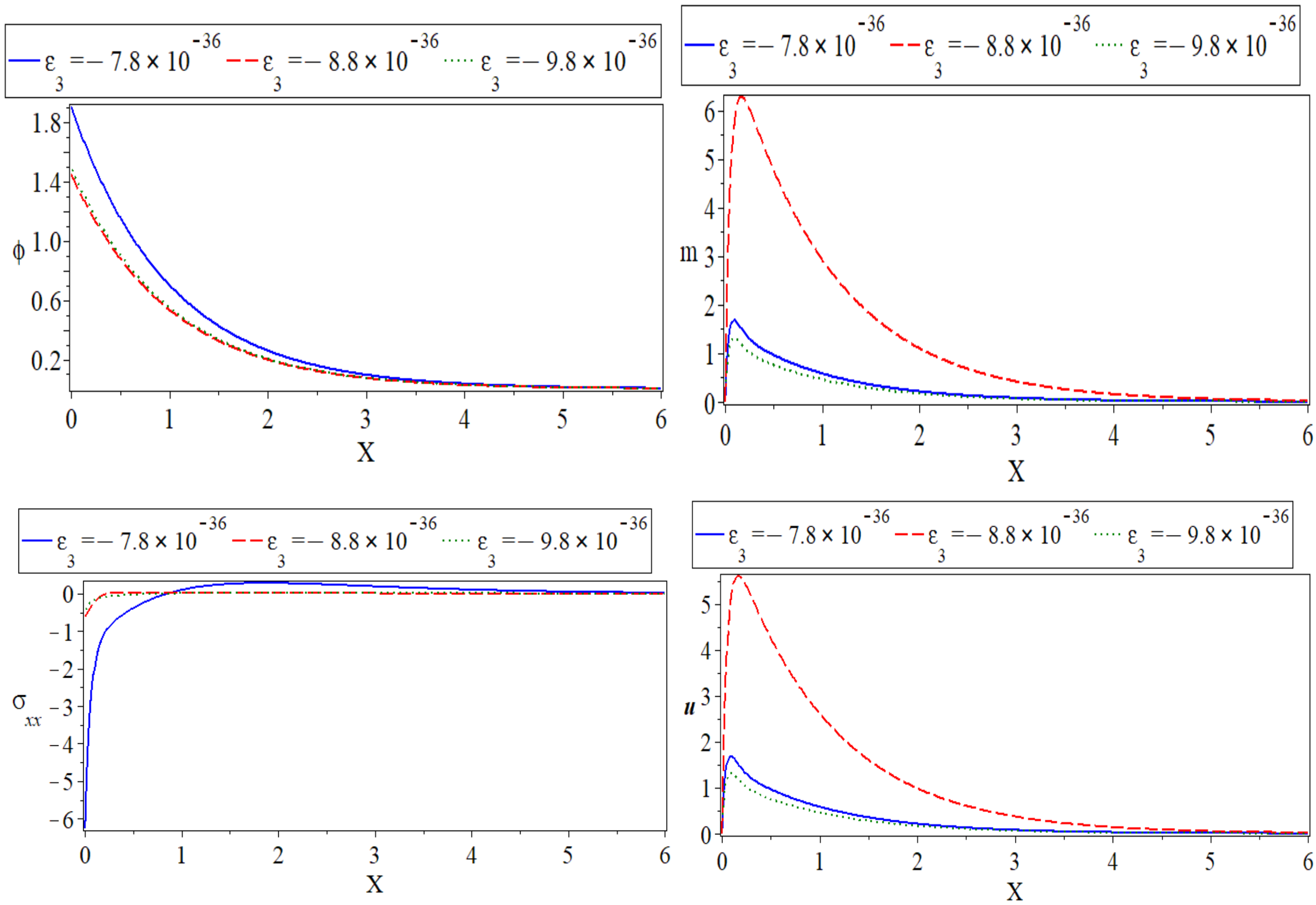

Figure 2. The variation of physical field distributions with distance at different values of thermoelectric coupling parameter ε_3 under the effect of moisture and $\varepsilon_1 = 0.001$.

6.3. The Effect of the Thermoelectric Coupling Parameter

The main physical fields are depicted in Figure 3 (third category) versus a horizontal distance within the setting of the photo-thermoelasticity theory with moisture diffusivity inside the two-temperature theory. All calculations are carried out with the impact of the moisture diffusivity when $\varepsilon_1 = 0.001$ and $m_0 = 10\%$ for Si materiel. All subfigures discuss three cases of the thermoelectric coupling parameter. The solid lines (————) represent the case when $\varepsilon_3 = -7.8 \times 10^{-36}$, the dashed lines (— — —) express the case at $\varepsilon_3 = -8.8 \times 10^{-36}$, and the dotted lines (⋯⋯⋯) show the case at $\varepsilon_3 = -9.8 \times 10^{-36}$. The thermo-dynamical temperature distribution with variation in the dimensionless thermoelectric coupling parameters with distance is shown in the first subfigure. Starting at a positive minimum value that satisfies the thermally insulated requirement, the thermodynamic temperature rises quickly in the first range until it reaches the peak maximum value close to the surface because of photo-excitation and moisture diffusivity. The distribution, on the other hand, contracts in the second range to approach the minimum value far from the surface. The carrier density distribution is shown against the distance in variation values of the thermoelastic parameters in the second subfigure. However, the carrier density, which exhibits a similar quality characteristic, is not significantly affected by a slight change in the thermoelastic coupling parameters. The conductive temperature, which behaves similarly to the dynamical temperature, is depicted in the third subfigure. The distribution of moisture concentration *m* against horizontal distance *x* is shown in the fourth subfigure. For each of the three scenarios, the moisture concentration distribution starts from a positive value for all three cases. In the case of $\varepsilon_1 = 0.001$, the distribution takes the exponential behavior with smooth decreasing. Still, on the other hand, when $\varepsilon_1 = 0.002$ and $\varepsilon_1 = 0.003$, the distribution of moisture concentration decreases sharply near the surface, and it takes an exponential propagation behavior until it reaches a minimum value near the zero line due to moisture diffusivity. The fifth subfigure shows how the mechanical loads that tend to raise the value of the thermoelectric coupling parameters enhance the stress force σ amplitude. The displacement distribution u with horizontal distance caused by moisture diffusivity and the thermal impact of photothermal stimulation for the rough surface is shown in the sixth subfigure. For each of the three thermoelectric coupling parameter situations, the displacement distribution begins at zero, climbs to maximum values near the surface, and then decreases in an exponential propagation pattern until it reaches a minimum value close to the zero line.

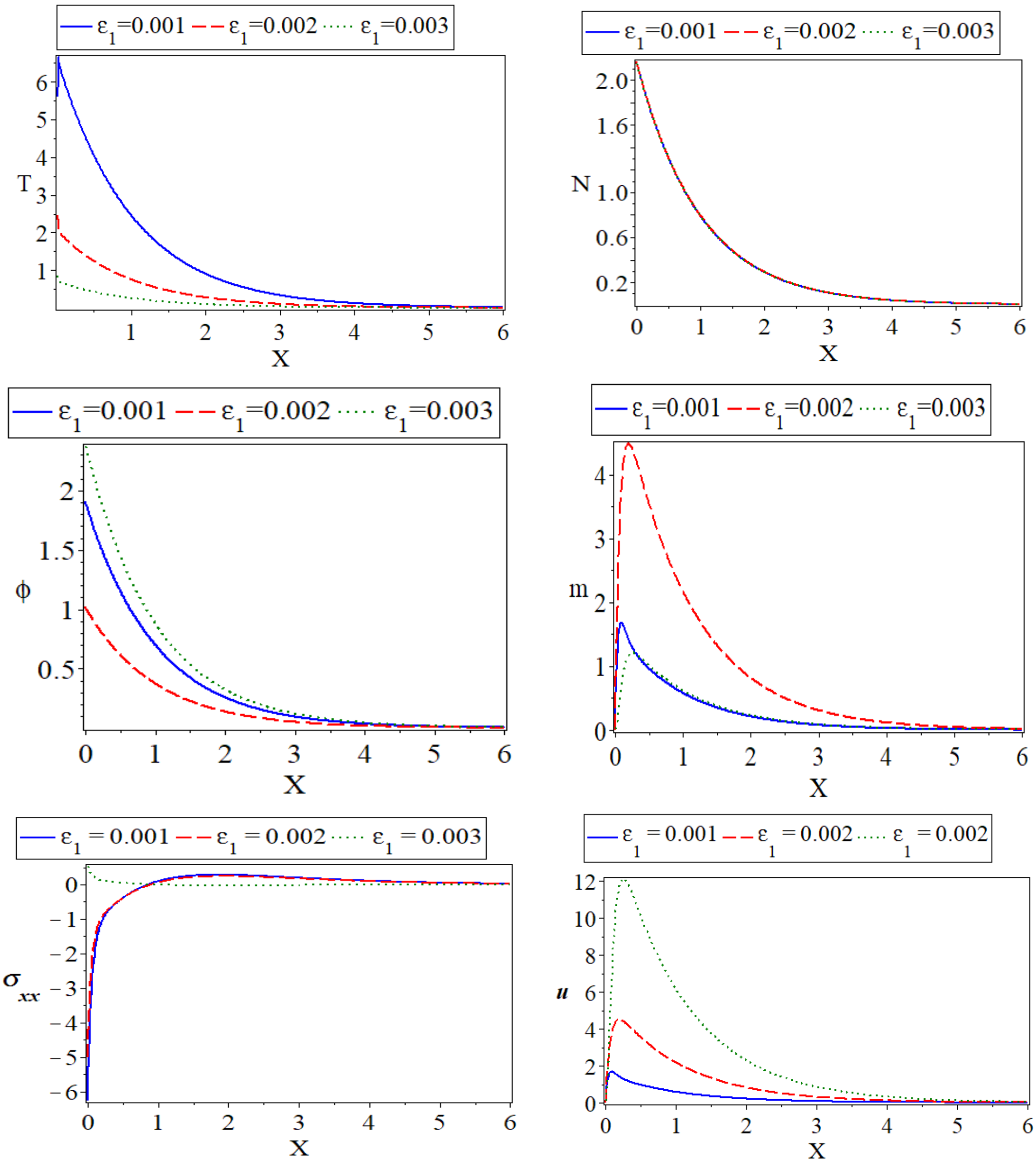

Figure 3. The variation of physical field distributions with distance at different values of thermoelastic coupling parameter ε_1 under the effect of moisture field and $\varepsilon_3 = -7.8 \times 10^{-36}$.

6.4. Influence of Reference Moisture

Figure 4 (fourth category) shows the principle physical fields against the distance x with moisture parameter. All calculations are carried out under the thermoelastic couples $\varepsilon_1 = 0.001, \varepsilon_3 = -7.8 \times 10^{-36}$ for Silicon (Si) material. Three cases of reference moisture m_0 are shown in Figure 4 with different physical field variations in relation to distance. The first represents the case of reference moisture when $m_0 = 10\%$ (————), the second case of reference moisture field when $m_0 = 20\%$ (— — —), and the third case of reference moisture field when $m_0 = 30\%$ (··········). All evaluations are made in the moisture field when $\varepsilon_1 = 0.001$ and $\varepsilon_3 = -7.8 \times 10^{-36}$. From this figure, it is clear that the moisture field affects the wave propagation behavior of displacement, moisture concentration, stress force, temperature distributions, and carrier density distribution, but carrier density does not affect it.

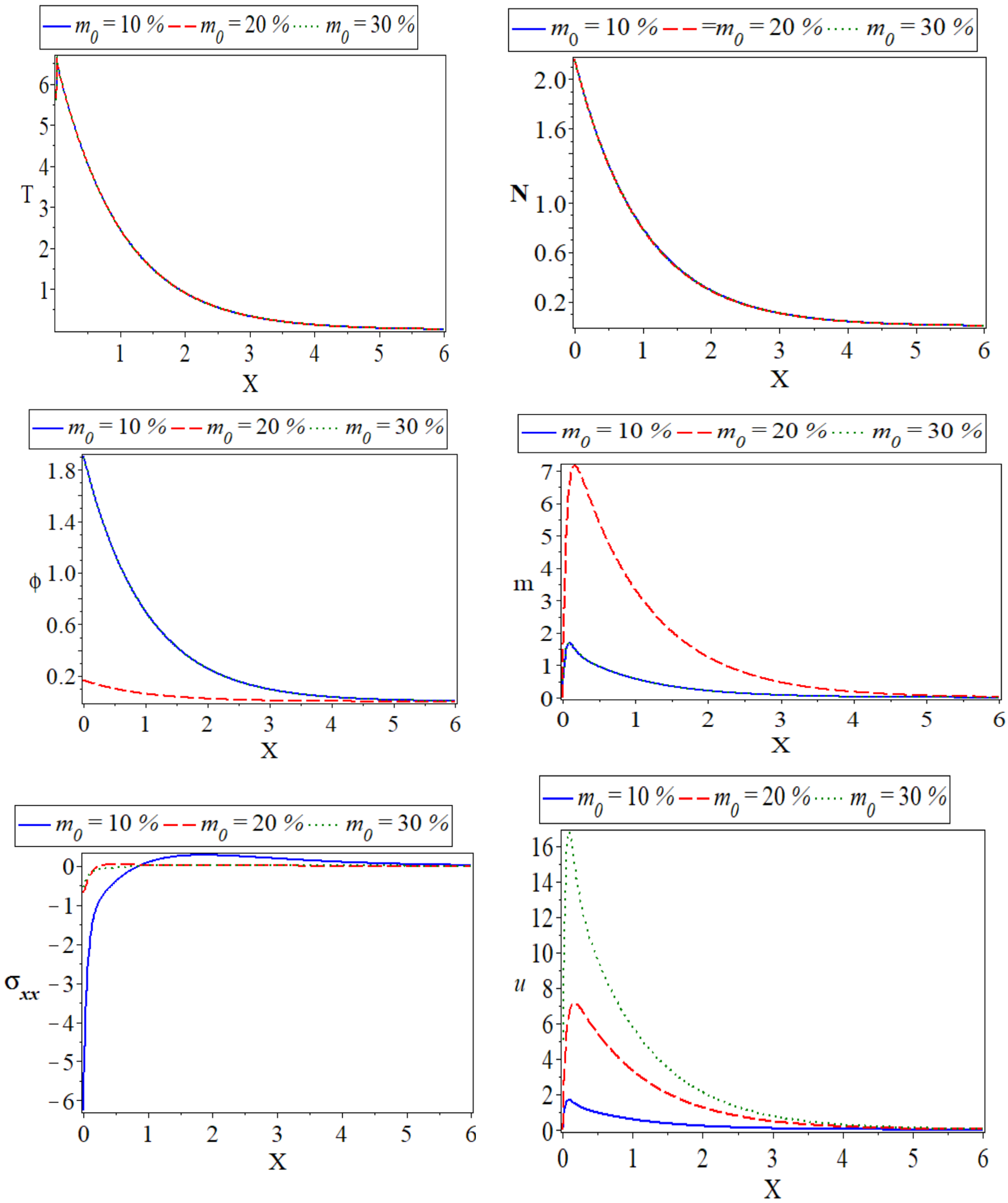

Figure 4. The variation of physical field distributions with distance at different values of the reference moisture m_0 under the effect of magnetic field when $\varepsilon_1 = 0.001$ and $\varepsilon_3 = -7.8 \times 10^{-36}$.

6.5. The Comparison between Si and Ge Materials

The comparison between the elastic semiconductor materials silicon (Si) and germanium (Ge) is shown in Figure 5 (the fifth category). The values of the physical fields in this problem have been evaluated numerically when $\varepsilon_1 = 0.001$ and $\varepsilon_3 = -7.8 \times 10^{-36}$ under the influence of moisture field and the two-temperature parameter. According to this figure, the physical constant differences between Ge and Si materials have a significant impact on all wave propagation of the quantities T, m, u, σ s, and ϕ.

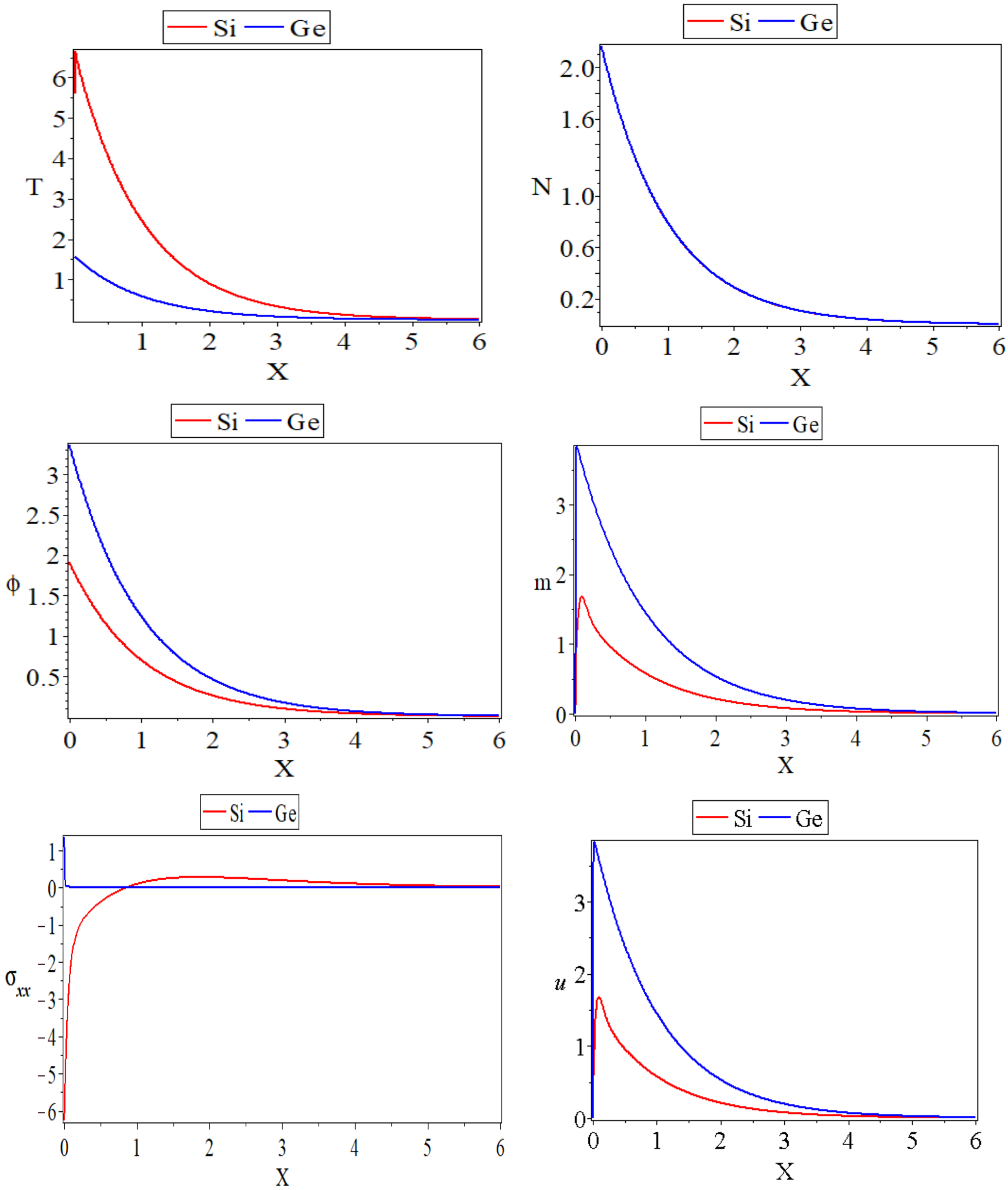

Figure 5. The comparison between Si and Ge materials of physical field distributions with distance under the effect of moisture field when $\varepsilon_1 = 0.001$ and $\varepsilon_3 = -7.8 \times 10^{-36}$.

7. Conclusions

The two-temperature and photo-thermoelasticity theories are taken into consideration in the innovative model that is explored in two dimensions. With some initial and boundary conditions, the complicated governing equations are assumed to be dimensionless. According to thermal relaxation times, the differences between photo-thermoelasticity theories are taken into account. For the fundamental parameters under consideration, the impacts of moisture diffusivity are clearly seen in the distributions of wave propagation. However, the two-temperature parameter also has a significant influence on all wave propagations. It is observed that changes in the two-temperature parameters have a considerable impact on silicon semiconductor wave propagation. On the other hand, the model employed is extremely helpful for researchers and engineers working in the field of renewable energy in terms of enhancing the performance of solar cells, electrical circuits, and computer processors.

Author Contributions: K.L.: Conceptualization, Methodology, Software, Data curation. E.S.E. and A.A.: Writing—Original draft preparation. R.S.T.: Supervision, Visualization, Investigation. A.A.E.-B.: Software, Validation. All authors: Writing—Reviewing and Editing. All authors have read and agreed to the published version of the manuscript.

Funding: This research received no external funding.

Data Availability Statement: The information applied in this research is available from the author at request.

Conflicts of Interest: The authors declare no conflict of interest.

References

1. Lord, H.; Shulman, Y. A generalized dynamical theory of thermoelasticity. *J. Mech. Phys. Solids* **1967**, *15*, 299–309. [CrossRef]
2. Green, A.E.; Lindsay, K. Thermoelasticity. *J. Elast.* **1972**, *2*, 1–7. [CrossRef]
3. Dhaliwal, R.S.; Sherief, H.H. Generalized thermoelasticity for anisotropic media. *Q. Appl. Math.* **1980**, *38*, 1–8. [CrossRef]
4. Green, A.E.; Naghdi, P. A re-examination of the basic postulates of thermomechanics. *Proc. R. Soc. London. Ser. A Math. Phys. Sci.* **1991**, *432*, 171–194.
5. Green, A.E.; Naghdi, P. On undamped heat waves in an elastic solid. *J. Therm. Stress.* **1992**, *15*, 253–264. [CrossRef]
6. Green, A.E.; Naghdi, P. Thermoelasticity without energy dissipation. *J. Elast.* **1993**, *31*, 189–208. [CrossRef]
7. Chen, P.J.; Gurtin, M.E. On a theory of heat conduction involving two temperatures. *Z. Angew. Math. Und Phys. ZAMP* **1968**, *19*, 614–627. [CrossRef]
8. Chen, P.J.; Williams, W.O. A note on non-simple heat conduction. *Z. Angew. Math. Und Phys. ZAMP* **1968**, *19*, 969–970. [CrossRef]
9. Warren, W.E.; Chen, P.J. Wave propagation in the two temperature theory of thermoelasticity. *Acta Mech.* **1973**, *16*, 21–33. [CrossRef]
10. Singh, M.; Kumari, S. Influence of gravity and initial stress on Rayleigh wave propagation in magneto-thermoelastic medium. *J. Math. Comput. Sci.* **2021**, *11*, 2681–2698.
11. Youssef, H.M. Theory of two-temperature-generalized thermoelasticity. *IMA J. Appl. Math.* **2006**, *71*, 383–390. [CrossRef]
12. Ezzat, M.A.; El-Karamany, A.S.; Ezzat, S.M. Two-temperature theory in magneto-thermoelasticity with fractional order dual-phase-lag heat transfer. *Nucl. Eng. Des.* **2012**, *252*, 267–277. [CrossRef]
13. Shivay, O.N.; Mukhopadhyay, S. On the temperature-rate dependent two-temperature thermoelasticity theory. *J. Heat Transf.* **2020**, *142*, 022102. [CrossRef]
14. Bajpai, A.; Kumar, R.; Sharma, P.K. Analysis of wave motion and deformation in elastic plate based on two temperature theory of thermoelasticity. *Waves Random Complex Media* **2021**, 1–22. [CrossRef]
15. Abouelregal, A.E.; Alanazi, R. Fractional Moore-Gibson-Thompson heat transfer model with two-temperature and non-singular kernels for 3D thermoelastic solid. *J. Ocean. Eng. Sci.* 2022, *in press*. [CrossRef]
16. Sharma, J.N.; Sharma, Y.D.; Sharma, P.K. On the propagation of elasto-thermodiffusive surface waves in heat-conducting materials. *J. Sound Vib.* **2008**, *315*, 927–938. [CrossRef]
17. Aouadi, M.; Moulahi, T. Asymptotic analysis of a nonsimple thermoelastic rod. *Discret. Contin. Dyn. Syst.-S* **2016**, *9*, 1475. [CrossRef]
18. Lotfy, K.; Hassan, W. Normal mode method for two-temperature generalized thermoelasticity under thermal shock problem. *J. Therm. Stress.* **2014**, *37*, 545–560. [CrossRef]
19. Kumar, R.; Gupta, V. Wave propagation at the boundary surface of an elastic and thermoelastic diffusion media with fractional order derivative. *Appl. Math. Model.* **2015**, *39*, 1674–1688. [CrossRef]

20. Kumar, R.; Kansal, T. Propagation of Rayleigh waves on free surface of transversely isotropic generalized thermoelastic diffusion. *Appl. Math. Mech.* **2008**, *29*, 1451–1462. [CrossRef]
21. Kumar, R.; Kansal, T. Effect of rotation on Rayleigh waves in an isotropic generalized thermoelastic diffusive half-space. *Arch. Mech.* **2008**, *60*, 421–443.
22. Kumar, R.; Kansal, T. Dynamic problem of generalized thermoelastic diffusive medium. *J. Mech. Sci. Technol.* **2010**, *24*, 337–342. [CrossRef]
23. Kumar, R.; Gupta, V. Problem of Rayleigh Wave Propagation in Thermoelastic Diffusion. *J. Solid Mech.* **2016**, *8*, 602–613.
24. Ezzat, M.A.; Abd Elall, M.Z. Generalized magneto-thermoelasticity with modified Ohm's law. *Mech. Adv. Mater. Struct.* **2010**, *17*, 74–84. [CrossRef]
25. Othman, M.I.A.; Lotfy, K. On the Plane Waves in Generalized Thermomicrostretch Elastic Half-space. *Int. Commun. Heat Mass Transf.* **2010**, *37*, 192–200. [CrossRef]
26. Othman, M.I.; Lotfy, K.; Farouk, R. Generalized thermo-microstretch elastic medium with temperature dependent properties for different theories. *Eng. Anal. Bound. Elem.* **2010**, *34*, 229–237. [CrossRef]
27. Lotfy, K.; Othman, M. The effect of rotation on plane waves in generalized thermo-microstretch elastic solid with one relaxation time for a mode-I crack problem. *Chin. Phys. B* **2011**, *20*, 074601. [CrossRef]
28. Lotfy, K. Mode-I crack in a two-dimensional fibre-reinforced generalized thermoelastic problem. *Chin. Phys. B* **2012**, *21*, 014209. [CrossRef]
29. Othman, M.; Lotfy, K. The effect of magnetic field and rotation of the 2D problem of a fiber-reinforced thermoelastic under three theories with influence of gravity. *Mech. Mater.* **2013**, *60*, 120–143. [CrossRef]
30. Lotfy, K.; Hassan, W.; El-Bary, A.; Kadry, M. Response of electromagnetic and Thomson effect of semiconductor mediu due to laser pulses and thermal memories during photothermal excitation. *Results Phys.* **2020**, *16*, 102877. [CrossRef]
31. Youssef, H.; El-Bary, A. Theory of hyperbolic two-temperature generalized thermoelasticity. *Mater. Phys. Mechs.* **2018**, *40*, 158–171.
32. Fahmy, M.A. Boundary element modeling of 3T nonlinear transient magneto-thermoviscoelastic wave propagation problems in anisotropic circular cylindrical shells. *Compos. Struct.* **2021**, *27*, 114655. [CrossRef]
33. Fahmy, M.A.; Almehmadi, M.M.; Subhi, F.M.; Sohail, A. Fractional boundary element solution of three-temperature thermoelectric problems. *Sci. Rep.* **2022**, *2*, 6760. [CrossRef]
34. Fahmy, M.A. 3D Boundary Element Model for Ultrasonic Wave Propagation Fractional Order Boundary Value Problems of Functionally Graded Anisotropic Fiber-Reinforced Plates. *Fractal Fract.* **2022**, *6*, 247. [CrossRef]
35. Fahmy, M.A.; Alsulami, M.O. Boundary Element and Sensitivity Analysis of Anisotropic Thermoelastic Metal and Alloy Discs with Holes. *Materials* **2022**, *15*, 1828. [CrossRef] [PubMed]
36. Fahmy, M.A. Boundary element modeling of fractional nonlinear generalized photothermal stress wave propagation problems in FG anisotropic smart semiconductors. *Eng. Anal. Bound. Elem.* **2022**, *134*, 665–679. [CrossRef]
37. Hosseini, S.M.; Sladek, J.; Sladek, V. Application of meshless local integral equations to two dimensional analysis of coupled non-Fick diffusionelasticity. *Eng. Anal. Bound. Elem.* **2013**, *37*, 603–615. [CrossRef]
38. Abo-Dahab, S.; Lotfy, K. Two-temperature plane strain problem in a semiconducting medium under photothermal theory. *Waves Random Complex Media* **2017**, *27*, 67–91. [CrossRef]
39. Lotfy, K.; Sarkar, N. Memory-dependent derivatives for photothermal semiconducting medium in generalized thermoelasticity with two- Temperature. *Mech. Time-Depend. Mater.* **2017**, *21*, 519–534. [CrossRef]
40. Lotfy, K.; Elidy, E.S.; Tantawi, R.S. Photothermal Excitation Process during Hyperbolic Two-Temperature Theory for Magneto-Thermo-Elastic Semiconducting Medium. *Silicon* **2021**, *13*, 2275–2288. [CrossRef]
41. Lotfy, K.; Elidy, E.S.; Tantawi, R.S. Piezo-photo-thermoelasticity transport process for hyperbolic two-temperature theory of semiconductor material. *Int. J. Mod. Phys. C* **2021**, *32*, 2150088. [CrossRef]
42. Xiao, Y.; Shen, C.; Zhang, W.B. Screening and prediction of metal-doped α-borophene monolayer for nitric oxide elimination. *Mater. Today Chem.* **2022**, *25*, 100958. [CrossRef]
43. Liu, J.; Han, M.; Wang, R.; Xu, S.; Wang, X. Photothermal phenomenon: Extended ideas for thermophysical properties characterization. *J. Appl. Phys.* **2022**, *131*, 065107. [CrossRef]